Evaluation of In Vitro and Anti-inflammatory Activity of Products Containing a Breath Mask and Filter Based on Polyurethane and Polyvinylidene Fluoride Nanofibers

Kyu oh Kim *

Posted Date: 31 October 2023

doi: 10.20944/preprints202310.2000.v1

Keywords: Nanofiber (NF); cytotoxicity; polyurethane (PU); polyvinylidene fluoride (PVDF); DMSO stocks; nitric oxide production; protein expression

Article

Evaluation of In Vitro and Anti-Inflammatory Activity of Products Containing a Breath Mask and Filter Based on Polyurethane and Polyvinylidene Fluoride Nanofibers

Kyu oh Kim [1,*]

[1] Department of Fiber System Engineering, Dankook University, 152, Jookjeon-ro, Suji-gu, Yongin-si, Gyeonggi-do, 448-701, Republic of Korea 1; affablekim@gmail.com (K.O. KIM)

* Correspondence: affablekim@gmail.com (K.O. KIM)

Abstract: Nanofiber (NF) products exhibit outstanding performances in the materials science, textile, and medical fields, which cannot be realized using conventional technologies. However, the safety of such products is debated because of the potential risk of nanomaterials and lack of standardized guidelines for safely evaluating NF products. The global safety evaluations of nanomaterials focused on evaluating the cytotoxicity of zero-dimensional materials including nanoparticles and nanotubes based on OECD criteria. The NFs are one-dimensional materials with nanometer diameters and considerable lengths. Many fibers are applied in a densely woven web-like form, and therefore, assessing cellular penetration and fiber toxicity using the same methods is inappropriate. This study verifies the safety of polyurethane (PU) and polyvinylidene fluoride (PVDF) polymers, which are currently applied in filters and masks. To this end, polymer NFs were collected from each product, and the NFs were compared with reference samples considering their physical properties using FT-IR and Raman spectroscopy. For the safety evaluation, DMSO stocks of varying concentrations of PVDF and PU NFs (at 0.5, 1, 5, and 10 μg/mL) were prepared, and the cytotoxicity and inhibitory effects on nitric oxide production and protein expression obtained via Western blot were identified.

Keywords: Nanofiber (NF); cytotoxicity; polyurethane (PU); polyvinylidene fluoride (PVDF); DMSO stocks; nitric oxide production; protein expression

1. Introduction

Nanoparticles have diameters ranging from 1–100 nm, which are larger than atoms and smaller than cells. The nanoparticles are a very small unit, approximately 1/100,000 the size of human hair [1-2]. Thus, an identical material in the nano-size acquires unique properties such as increased strength or electrical conductivity. Nanomaterials can readily alter the electrochemical properties on their surfaces, and using this, a diversity of nanomaterials can be fabricated according to the purpose of use [3-4]. Thus, they have been applied in a variety of fields from chemical materials to automobiles, information and communications technology, environmental energy and biomedicine. Although nanomaterials are useful in daily life with their unique properties, the same properties have given rise to nanohazards. Owing to their small size, nanomaterials can more easily penetrate the human body and induce toxicity with a greater probability [5-10]. The diagnosis of safety is critical because the cytotoxic potential of nanomaterials may vary according to various changes in physicochemical properties. Nanofibers (NFs) defined as a type of nanomaterials comprise organic polymers in a 2D membrane form [11].

The most representative method for fabricating nanoscale NFs is electrospinning, which is a technique developed in the early 20th century that has been most notably applied in the filtration industry [12]. Electrospinning is a simple and rapid high-performance technique used for fabricating NFs using polymers. The technique applies a strong electromagnetic force at ~20–30 kV for ionizing a polymer solution. The device has a polymer solution on one side and its opposite charge on the other so that a narrow jet of polymer solution called Taylor cone is formed because polymer solutions

 doi:10.20944/preprints202310.2000.v1

tend to migrate towards opposite charge, which leads to the formation of 1D fibers in nanoscale diameters. The formation of a membrane with large surface areas and porosity can be applied in high-performance filters, sensor components, biomaterials, and electrode separators [13 - 23]. However, a standard method for verifying the effects of the currently manufactured and commercialized NF products on the human body and determining potential hazards is lacking, and only few studies have investigated the host response at the interface generated when NFs enter and accumulate in the human body. This raised the need for research on evaluating the safety of NF products.

This study conducted a cytotoxicity assay using a cell line for validation prior to clinical trials for determining the effects of wearing a mask containing NFs on the human respiratory system [24, 25]. A cytotoxicity assay is a biological assessment of safety for determining nontoxic biocompatible compounds. An *in vitro* analysis precedes an *in vivo* analysis based on rapid results and reproducibility, and *in vitro* assays are widely used as a pre-validation test with advantages of reduced number of animals in subsequent animal studies and increased clinical accessibility such as defining the concentrations of compounds. Cytotoxicity assays are a type of biological assessments and screening tests, whereby cellular growth, regeneration, and morphological changes are examined and evaluated. Among the various evaluation methods, the MTT assay with its wide spectrum of use has been applied for testing the cytotoxicity in this study.

Inflammation is a natural biological response to human tissue damage induced by various stimuli from infection to chemical substances and immune responses. Macrophages play central roles in inflammatory responses, and through their phagocytosis, cytotoxicity, and cell killing ability, they play a key role in the defense mechanism of the host. Lipopolysaccharides (LPSs) are generated in the cell walls of Gram-negative bacteria with a powerful ability to induce inflammatory cytokines [26, 27]. The LPS activity increases the production of inflammatory mediators such as nitric oxide (NO), tumor necrosis factor-α (TNF-α), interleukin (IL), prostaglandin (PG), and leukotriene. LPS-activated RAW 264.7 macrophages are widely used in exploring anti-inflammatory materials. Upon LPS stimulation, RAW 264.7 cells increase the secretion of cytokines such as IL-1β, IL-6, TNF-α, and NO. The production of NO employs nitric oxide synthase (NOS) and L-arginine substrate. The important roles of NOS includes the control of vascular tone, neurotransmission, microbial removal, and homeostatic mechanisms. Inducible NOS (iNOS) is expressed upon stress or via inflammatory cytokines such as IL-1β, IL-6, and TNF-α; these cytokines activate macrophages and act as mediators for inducing acute and chronic inflammatory responses. Therefore, controlling such inflammatory cytokines and various mediators is critical for developing drugs for various inflammatory diseases, although they may also be key targets in creating anti-inflammatory materials.

This study verified the safety of the commercialized PVDF and PU NFs in currently available filters and masks. To this end, NFs were collected from sample products, and their physical properties were evaluated using Fourier transform infrared (FT-IR) and Raman spectroscopy. Cytotoxicity assay and anti-inflammatory investigation were conducted for a safety evaluation. The results confirm the anti-inflammatory effects of NF products and present the potential applicability of NFs as functional materials. These results provide basic data that can be applied to several different fields.

2. Materials and Methods

2.1. Materials

Electrospun polyvinylidene difluoride (PVDF or PVDF NFs) for a breath mask and PU (or PU NFs) for the breathable water-proof membrane was purchased from Lemon Corporation (Gumi, Korea). The physical properties are summarized in Table 1. All samples were air dried prior to characterization.

Table 1. Physical properties of PVDF and PU nanofibers.

Preprints (www.preprints.org) | NOT PEER-REVIEWED | Posted: 31 October 2023 doi:10.20944/preprints202310.2000.v1

Physical property (unit)	PVDF	PU	Test method
Basic weight (g/m²)	4.1	3.8	ASTM D 3776
Air permeability (cm³/cm²/s)	1.02	1.2	ASTM D 737
Thickness (μm)	7.9	6	ASTM D 1777
Hydrostatics (mmH_2O)	700	5,000	AATCC 127
Color	white	white	

SEM image

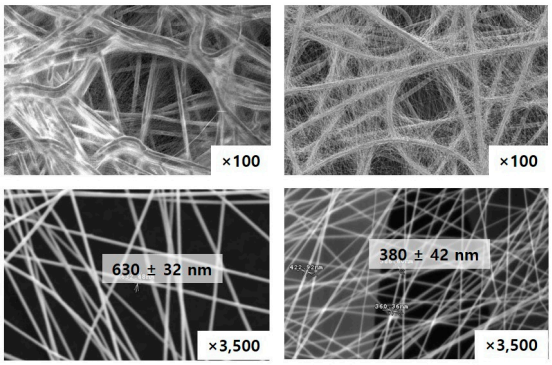

2.2. Fourier-Transform Infrared Spectroscopy

FT-IR spectra analysis was conducted using a Perkin Elmer Spectrum II (Manufacturer Model, Location) for confirming the structural analysis of the PVDF NFs and PU NFs. The FTIR spectra were obtained from KBr pellets, and they were made by mixing KBr powder and the sample at a ratio of about 100:1 using agate induction so that it is well dispersed, and then, making a pellet by applying pressure on a pellet molding apparatus. The sample was analyzed in the range of 4000–400cm^{-1} to confirm the presence of the characteristic peaks of the PVDF and PU NFs and the changes in peak positions and shapes.

2.3. Raman Spectroscopy

Raman spectra were recorded with a Bruker IFS 100 Fourier transform Raman spectrometer equipped with an air-cooled Nd:YAG laser source (514.5 nm) with an output power of 30–200 mW and a Ge detector cooled by liquid nitrogen. A laser beam with 200 mW power, as monitored at the base of a quartz plate supporting PVDF and PU NFs, was used for Raman measurement.

2.4. Cell Viability

The commercially available research materials necessary for the study include reagents such as 3-(4,5-dimethythiazol-2-yl)-2,5-diphenyl tetrazolium bromide (MTT), dimethyl sulfozide (DMSO), LPS, recombinant human TNF-α (rhTNF-α), and ELISA reader (BioTek). The dissolution was most efficient in DMSO when PU and PVDF NFs were tested in several solvents. Therefore, DMSO stocks with varying concentrations of PU and PVDF NFs (0.5, 1, 5, and 10 μg/mL) were prepared, and an equal amount of each stock was used in the cellular assay. The human immortalized keratinocyte cell line (HaCaT) was widely used in skin physiology and differentiation studies. Further, HaCaT cells were obtained from a government research center and the experiment was conducted with relatively short (~10) passages [28]. The Raw 264.7 (RAW) cell line is derived from BALB/c mice infected with Abelson leukemia virus, which is popular as a monocyte/macrophage model [29]. RAW cells were obtained from the Korean Cell Line Bank (KCLB), and cells with short (~10) passages were applied in the experiment. The two types of cells were cultured in Dulbecco's Modified Eagle's medium (DMEM) containing 10% fetal bovine serum (FBS) and 1% antibiotics (10,000 μg/mL streptomycin

 doi:10.20944/preprints202310.2000.v1

and 10,000 units/mL penicillin) in a 37 °C, 5% CO_2 incubator. The cells were passaged every two to three days.

An MTT assay was conducted to measure cell viability. In an MTT assay, which relies on the ability of the dehydrogenase in cellular mitochondria to convert tetrazolium, a soluble, yellow substrate, into insoluble, blue-violet formazan, the absorbance indicates the amount of reduced formazan in proportion to the number of cells in each well. Cells in the MTT assay were seeded at 1−2 × 10^5/mL by counting only the viable cells after the treatment with 0.4% trypan blue. A hemacytometer was used in cell counting. At confluency < ~80%, the cells were treated with NFs and LPS or TNF-α. After a 24 h culture, 40 μL of the culture solution was removed and 40 μL of 5 mg/mL MTT reagent was added for a 3 h culture [30]. The cells were dissolved in 40 μL of DMSO in a shaker for ~20 min after completely removing the supernatant. The absorbance was measured at 590 nm using an ELISA reader. Triplicate measurements were conducted for all test groups, and statistical significance was tested using Student's t-test with the level of significance set at $p < 0.05$ [31].

2.5. Inhibitory Effects on Nitric Oxide (NO) Production

The mouse macrophages RAW 264.7 cells were cultured in DMEM (HyClone, PA, USA) containing 10 % heat-inactivated FBS (HyClone, PA, USA) and 100 U/mL penicillin/streptomycin (HyClone, PA, USA) in a 37 °C, 5 % CO_2 incubator.

The level of NO_2 present in the culture solution was measured using the Griess reagent to measure the amount of NO produced from RAW 264.7 cells. After seeding RAW 264.7 cells in a 6-well plate at 5 × 10^5 cell/well, the cells were cultured in a 37 °C 5% CO_2 incubator for 24 h. Next, the cells were washed twice with 1 × PBS and treated with 1 μg/mL of LPS with the exception of the control group. After 1 h, the cells were treated with varying concentrations of samples solutions, and the supernatant was collected after a 24 h culture. An equal amount of the Griess reagent was added for a 10 min reaction in a 96-well plate, and the absorbance was measured at 540 nm. The inhibitory effects on NO production were expressed as the rate of reduction in absorbance for the sample and nonsample groups.

2.6. Western Blot

RAW 264.7 cells were seeded in a 6-well plate at 5 × 10^5 cell/well and stabilized through 24 h culturing to examine the iNOS and COX-2 activities. The cells were treated with 1 μg/mL of LPS and subsequently with culture medium with varying concentrations of NFs after removing the medium. After a 24 h culture, the medium was removed and the cells were washed twice with PBS. Then, the cells were dissolved in 100 μL of a 10 mL solution of radio-immunoprecipitation assay (RIPA) buffer with complete mini 1 tab, followed by 20 min centrifugation at 4 °C and 16,110 × g. The resulting supernatant was quantified using a BCA protein assay kit and 20 μL of the collected proteins were electrophoresed using 10% SDS-PAGE. The separated proteins were transferred to the PVDF NFs and left in a blocking buffer (5% skim milk in TBST) at 25°C for 1 h. The diluted primary antibodies of iNOS, COX-2, and β-actin were applied at 4 °C overnight followed by three times washing with tris-buffered saline and tween 20 (TBST) in 10 min intervals. The secondary antibodies, anti-rabbit for iNOS and COX-2, and anti-mouse for β-actin, were diluted at 1:1,000 for a 2 h reaction at room temperature. The bands were identified and quantified using an LAS 4,000 device after three times washing with TBST.

3. Results and Discussion

3.1. Spectroscopic Investigation of Electrospun PVDF and PU Nanofibers

Table 1 lists the physical properties of the two different NFs used in this study. PVDF and PU NFs were analyzed using FT-IR and Raman spectroscopy to suggest two methods for evaluating the level of NFs dissociating from a NF product and entering the human body through the respiratory tract or other routes. Every molecule vibrates at a unique frequency. Applying light at a frequency equivalent to the vibration frequency of the molecule increases the vibration to cause special

Preprints (www.preprints.org) | NOT PEER-REVIEWED | Posted: 31 October 2023 doi:10.20944/preprints202310.2000.v1

phenomena including absorption or significant scattering of light. In other words, the identity of the molecule can be deduced if such special phenomena are detected upon applying light at a specific frequency to a given molecule. Figure 1 shows the PVDF and PU NF particles after grinding and the comparison between each respective reference line.

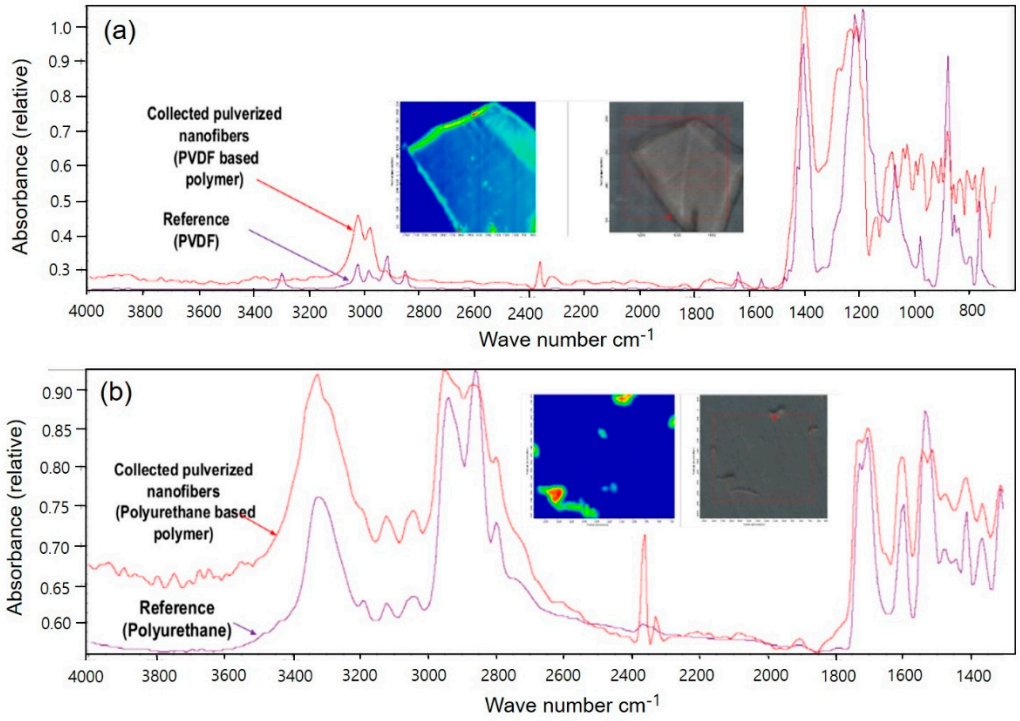

Figure 1. FT-IR spectra for (a) PVDF, (b)PU reference and nanofibers.

For PVDF, the most representative peaks were as follows: The characteristic absorption band of PVDF α-phase at 1,072 cm^{-1} and β-phase at 1,403 cm^{-1} (Figure 1A). The bands at 552 and 840 cm^{-1} are assigned to CF_2 bending and that at 796 cm^{-1} is assigned to the CF_2 skeletal vibrational mode. The bands at 796 and 839 cm^{-1} are attributed to CH_2 rocking. Splitting the band around 1,180 cm^{-1} results in stretching vibrations of CF [32-34]. Figure 1B shows the presence of the NH, C=O, C=C, and C-N peaks at 3,290, 1,704, 1,521, and 1,600 cm^{-1}, respectively, for PU.

The peaks of NF particles exhibit similar vibration behaviors to the reference peaks, as confirmed. In addition, a Raman spectrometer is used as the optical device for evaluating nanoparticles.

Figure 2 shows the Raman spectra for PVDF and PU. The PVDF spectra (Figure 2A) shows that the crystal form is the α-phase or form II characterized by chain conformation. PVDF modes are observed at 480 and 611 cm^{-1}. These modes are caused by CF_2 vibrations. The modes at 513 cm^{-1} attributed to the CF_2 bending vibration and higher intensity band at 840 cm^{-1} caused by out-of-phase combination of the CH_2 rocking and CF_2 stretching modes [35]. These modes are β-phase or form I of PVDF, and they are typical for the all-trans conformation of the PVDF chains. The all-trans conformations are attributed to the strain induced by swelling in the amorphous regions. The Raman spectrum of PU (Figure 2B) is characterized by three main urethane peaks: the C=O stretching vibration at 1,620 cm^{-1} and the N single-bond H stretching and C single-bond H bending vibrations at 1,450 and 1,320 cm^{-1}, respectively. The specific peaks of PVDF and PU NFs were identical to the reference peaks, and the potential use of the device in analyzing the dissociating nanoparticles was verified.

Preprints (www.preprints.org) | NOT PEER-REVIEWED | Posted: 31 October 2023 doi:10.20944/preprints202310.2000.v1

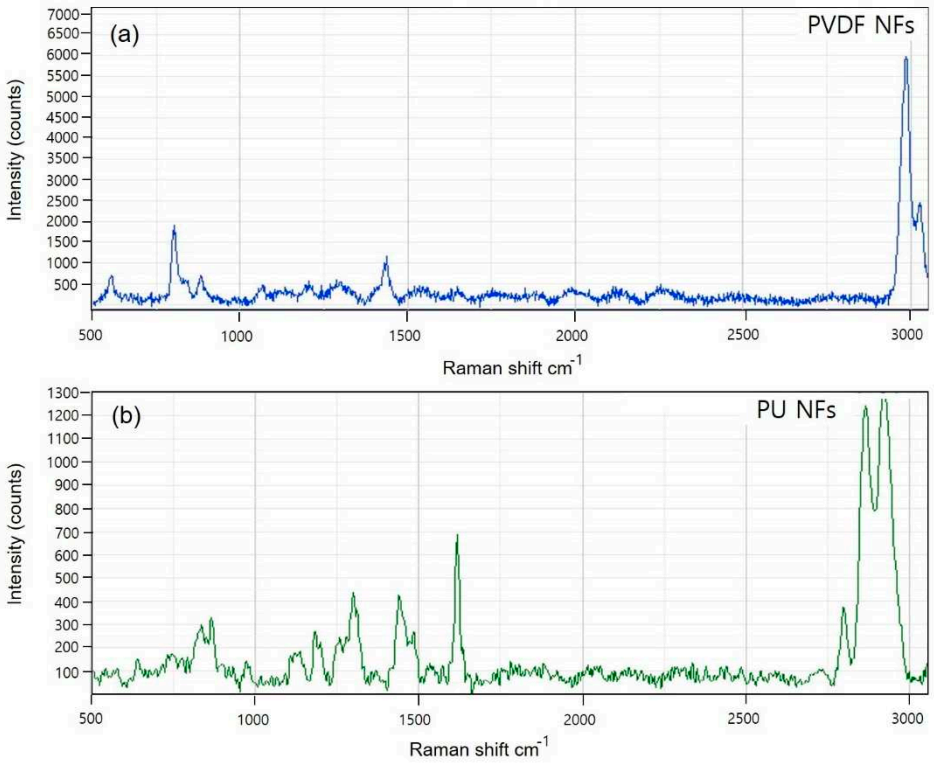

Figure 2. Raman spectrometer of PVDF and PU reference and nanofibers on the breath mask and filter.

3.2. Anti-Inflammatory Activity Investigation of PVDF and PU NFs

The result of the MTT assay demonstrated a concentration-dependent reduction in the LPS-treated groups of the two cells lines used as the positive control, compared to the that of the control group (ctrl) (Figure 3A). The LPS 5 μg/mL group showed a reduction to 77% and 84% growth in RAW and HaCaT cells, respectively, compared to that of the control. Therefore, 5 μg/mL was set as the level of LPS stimulation in subsequent experiments for examining changes in cell viability upon simultaneous treatment with NFs. No notable change in cellular growth is observed for HaCaT cells treated only with NFs (Figure 3D). In contrast, RAW cells treated only with PVDF NFs showed reduced cell viability, and those treated only with PU NFs showed significant overgrowth (Figure 3C). Groups treated with TNF-α as another positive control display the concentration-dependent reduction in cell viability (Figure 3B). As shown in Figure 3, the RAW cells treated only with PU NFs exhibit a higher level of cell viability compared to that for the control, whereas cells treated simultaneously with LPS and PU NFs exhibit a trend of further decrease in cell viability compared to those treated only with LPS. A significant concentration-dependent reduction in cell viability is observed for cells treated with LPS and PVDF NFs (Figure 4A). The viability of RAW cells decreases significantly upon treatment with 5 and 10 μg/mL of PVDF NFs following the treatment with TNF-α; however, the difference in comparison with the cells treated with only PVDF NFs is not significant (Figure 4C). The treatment with 1, 5, and 10 μg/mL of PU NFs significantly increases the cell viability compared to the cells treated with TNF-α only (Figure 4C). For HaCaT cells, slightly increased or similar cell viability is observed across most concentrations of NFs compared to cells treated only with LPS or TNF-α (Figure 4B and 4D).

Preprints (www.preprints.org) | NOT PEER-REVIEWED | Posted: 31 October 2023 doi:10.20944/preprints202310.2000.v1

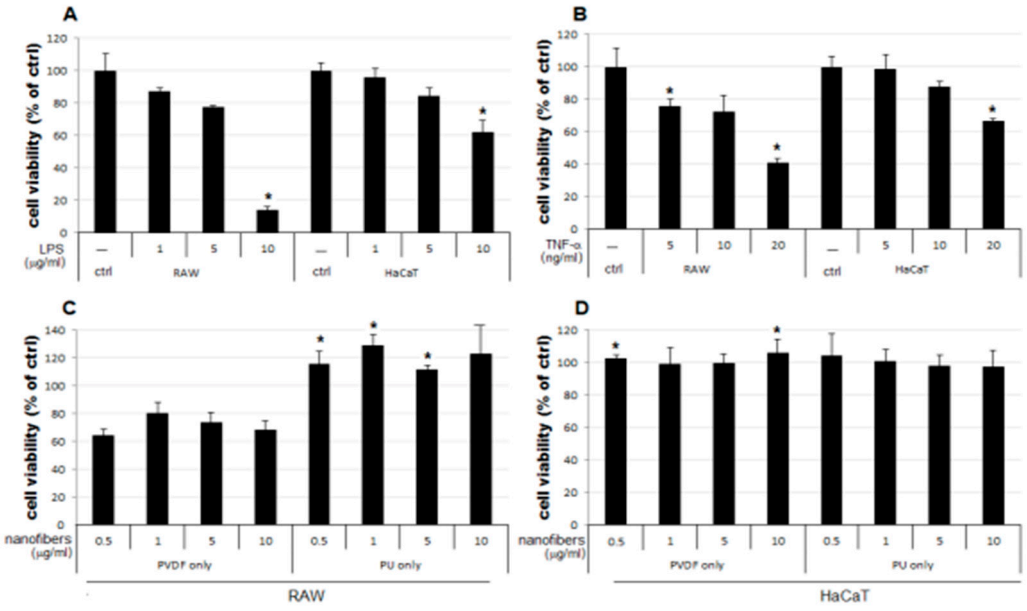

Figure 3. Results of cell viability with only PVDF NFs and PU NFs. Cell viability decreased by LPS or TNF-α in a dose-dependent manner (A and B). Graphs show results of the cell viability of nanofibers on raw and HaCaT cells (C and D). The results are expressed as the mean ± SEM. *P<0.05 vs non-treated cells.

LPS is a component of the outer membrane of Gram negative bacteria, and it is a well-known endotoxin that induces iNOS. This enzyme is responsible for producing various inflammatory cytokines and NO in macrophages, and it can increase the secretion of pro-inflammatory cytokines such as TNF-α, IL-1β, and IL-6 by stimulating macrophages or monocytes. Further, TNF-α is a cytokine produced in macrophages, lymphocytes, and leukocytes; it is not produced in a normal state, whereas its synthesis and secretion occur upon the stimulation of macrophages. The formation of NO plays a key role in the killing of bacteria or removal of tumors; however, the inflammatory response including edema and vascular permeability to NO produced by iNOS has been shown to promote inflammation. The genetic expression of proinflammatory proteins such as TNF-α, IL-1β, and IL-6 are regulated via the activation of nuclear factor kappa-light chain-enhancer of the activated B cells (NF-κB), which is a known transcription factor involved in inflammatory responses. NF-κB plays a crucial role in inflammatory responses by regulating the activation of iNOS. Assuming PU NFs play an inhibitory role in the synthesis of NO—a key mediator in LPS-mediated inflammation in RAW cells—it is necessary to determine changes in the amounts of cytokines that mediate inflammation (TNF-α, IL-1β, and IL-6) as inflammatory markers and verify changes in the amounts of iNOS and NF-κB proteins through Western blot analysis.

Preprints (www.preprints.org) | NOT PEER-REVIEWED | Posted: 31 October 2023 doi:10.20944/preprints202310.2000.v1

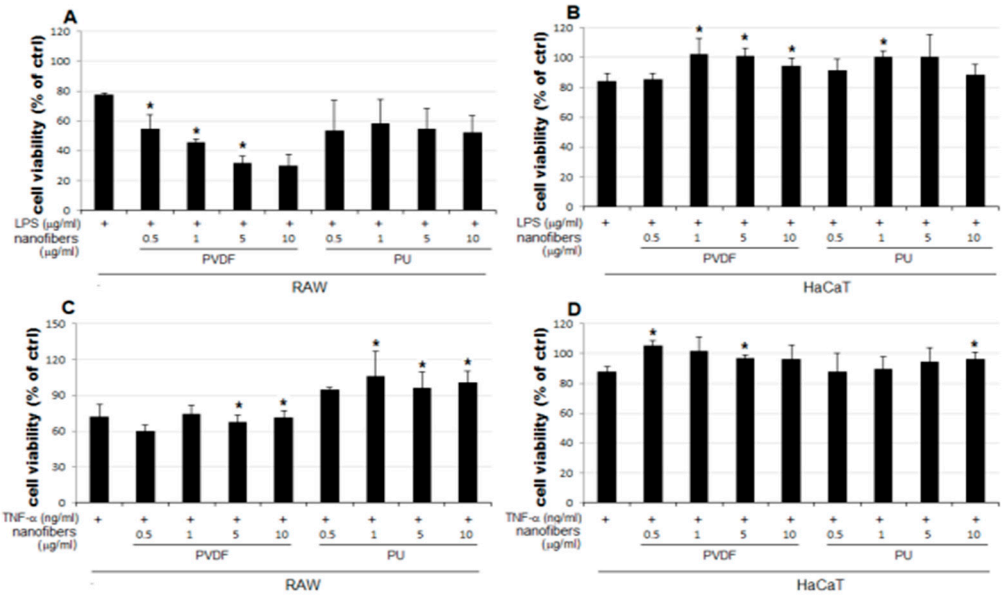

Figure 4. Results of the cell viability of NFs with LPS or TNF-α. HaCaT cells showed slightly higher cell viability with NFs than that with only stimuli (B and D). Cell viability are lowered with PVDF; however, in the case of PU, the cell viability was higher than the stimuli for only the treatment group (A and C). The results are expressed as the mean ± SEM. *P<0.05 vs cells treated with only LPS (Figure 4A and B) or only TNF-α (Figure 4C and D).

In this study, changes in cell viability upon the treatment with NFs were examined using RAW and HaCaT cells, following the LPS- or TNF-α-induced inflammatory response. The results are summarized as follows:

1. The cell viability is not significantly affected in HaCaT cells treated only with NFs (Figure 4D). The cell viability increases in cells simultaneously treated with LPS or TNF-α and PU or PVDF NFs (Figure 4B and 4D).

2. The cell viability decreases to 64−80% in RAW cells treated only with PVDF NFs (Figure 4C). For RAW cells, the simultaneous treatment with LPS or TNF-α and PVDF NFs led to a fall in cell viability. A significant reduction is observed upon simultaneous treatment with LPS and PVDF NFs in a concentration-dependent manner (Figure 4A).

3. The cell viability is at an excessive level in RAW cells treated with only PU NFs, whereas the simultaneous treatment with LPS and PU NFs does not increase cell viability (Figure 4A). Cells treated with TNF-α and PU NFs simultaneously show a significant increase in cell viability compared to those treated with only TNF-α (Figure 4B).

3.3. Inhibitory Effects of PVDF and PU NFs on Nitric Oxide Production

The effects of PU and PVDF NFs on NO production and their roles in inflammatory responses were determined. The MTT cytotoxicity assay demonstrated that the viability of RAW 264.7 cells decreased to 80% or lower after treatment with 5 μg/mL of PVDF NFs or 10 μg/mL of PU NFs. Thus, the final concentration of NO was set at 1 μg/mL and 5 μg/mL for PVDF and PU NFs, respectively. As shown in Figure 5, the level of NO expression in the LPS-treated group is higher compared to that of the control, whereas cells treated with PU or PVDF NFs exhibit reduced NO expression. The level of NO production was 38.0% at 5 μg/mL of PU NFs and 39.4% at 1 μg/mL of PVDF NFs, which indicated a 61.9% and 60.5% reduction, respectively. Inhibitory effects of PU and PVDF NFs on inflammatory responses were confirmed in RAW 264.7 cells. The safety of PU NFs was higher considering the low cell viability at low concentrations (0.1−1 μg/mL) of PVDF NFs in the previous cytotoxicity result.

Preprints (www.preprints.org) | NOT PEER-REVIEWED | Posted: 31 October 2023 doi:10.20944/preprints202310.2000.v1

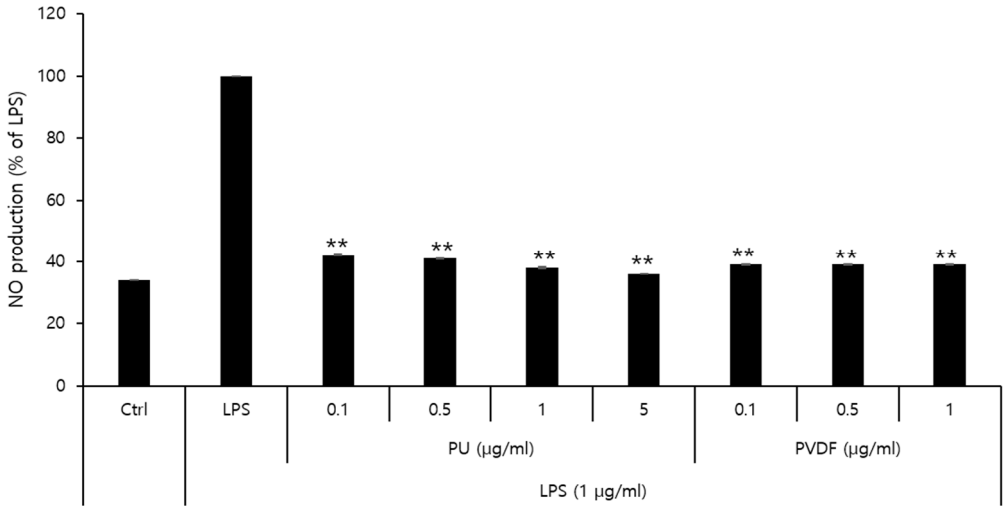

Figure 5. Effect of PU and PVDF NFs on NO production in LPS-induced RAW 264.7 cells. RAW 264.7 cells (5×10^5 cells) were treated with PU and PVDF NFs and LPS (1 μg/mL) for 24 h. A statistically significant difference versus LPS by ANOVA and Duncan's multiple range test (Significant as compared to control; $^{**}p < 0.01$).

3.4. Inhibitory Effects of PU NFs on iNOS and COX-2 Protein Expression

NO is an inflammatory marker synthesized by NOS using L-arginine. Three types of NOSs are present: endothelial NOS, neuronal NOS, and iNOS. The formation of NO by iNOS has an important pathological role. Another inflammatory marker, cyclooxygenase (COX), is an enzyme that converts arachidonic acid into prostaglandins. COX-1 and COX-2 with different patterns exist in different cells. Although COX-1 is involved in normal physiological functions in normal cells, COX-2 is expressed in the areas of inflammatory responses. Further, PGE_2 produced by COX-2 is an inflammatory mediator of pain and fever with a role in inflammatory and immune responses. This is closely related with angiogenesis. Western blot analysis was conducted to measure the inhibitory effects on the protein expression of iNOS and COX-2 as inflammatory markers. The macrophage RAW 264.7 cells were treated with varying concentrations (0.1, 0.5, 1, and 5 μg/mL) of PU NFs. The inhibitory effects on the protein expression after 24 h are measured and shown in Figure 6. The positive control was β-actin from a house keeping gene, whose expression rarely varies according to cell type or environment. Figure 6 shows that the protein expression of iNOS increased by LPS in RAW 264.7 cells decreased markedly to 24.6, 15.7, 13.6, and 12.1% after treatment with PU NFs at 0.1, 0.5, 1, and 5 μg/mL, respectively, in a concentration-dependent manner. At the same concentrations, the protein expression of COX-2 decreased to 79.8, 89.1, 64.9, and 70.6%, and the inhibition of protein expression was significant compared to the cells treated with LPS.

Preprints (www.preprints.org) | NOT PEER-REVIEWED | Posted: 31 October 2023 doi:10.20944/preprints202310.2000.v1

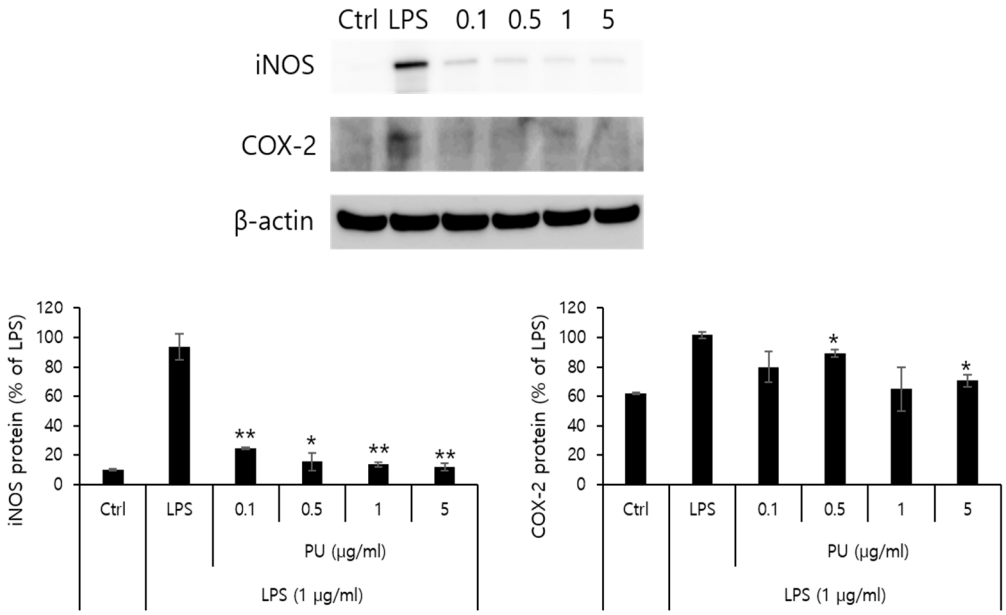

Figure 6. iNOS, COX-2 protein expression rate of PU NFs on macrophage cell (RAW 264.7). iNOS and COX-2 protein expression rates of PU NFs. After RAW 264.7 cells (5×10^5 cells) were started in a serum-free medium for 1 h, the cells were treated with 0.1, 0.5, 1, and 5 μg/mL of PU NFs for 24 h. Statistically significant differences versus LPS by ANOVA and Duncan's multiple range test. (Significant as compared to control. $^*p < 0.05$ $^{**}p < 0.01$).

4. Conclusion

NFs were collected from the available products and the potential use of FT-IR and Raman spectroscopy in NF evaluation was tested to verify the safety of PVDF and PU NFs in commercialized filters and masks. The cytotoxicity assay and anti-inflammatory investigation were used for the safety evaluation. The nanohazards were evaluated in accordance with the verified anti-inflammatory effects using NF products. The results are listed below:

1. The cell viability is unaffected in HaCaT cells treated with only NFs (Figure 4D). The cell viability increased in cells simultaneously treated with LPS or TNF-α and PU or PVDF NFs.
2. The treatment with PU and PVDF NFs was effective in inhibiting the expression of inflammatory mediators in RAW 264.7 cells.
3. The LPS-induced iNOS expression in RAW 264.7 cells decreased after treatment with PU NFs at 0.1, 0.5, 1, and 5 μg/mL, indicating a high level of inhibition in a concentration-dependent manner. The inhibition of COX-2 expression was observed at equal concentrations, whereas the level of inhibition was higher compared to cells treated with LPS.

Author Contributions: All research and experiments, writing-original draft were conducted entirely by K.O.KIM. For this experiment, data was provided by PH. D H.J. MOON, affiliated with KOTITI Research Institute, and Cell experiments were conducted with the help of. prof. J.T. KIM, Department of Cosmetology, Kyungsung National University.

Funding: This study was supported by the Technology Innovation Program (Nano product performance safety evaluation technology development and business support project) (20014731,development of safety evaluation method for nonwoven and garment products containing nanofiber) funded by the Ministry of Trade, Industry & Energy (MOTIE, Korea).

Institutional Review Board Statement: Not applicable.

Data Availability Statement: The data presented in this study are available on request from the corresponding author.

Acknowledgments: In this section, you can acknowledge any support given which is not covered by the author contribution or funding sections. This may include administrative and technical support, or donations in kind (e.g., materials used for experiments).

Conflicts of Interest: The author declares no conflict of interest.

References

1. Tiwari, J.N.; Tiwari, R.N.; Kim, K.S. Zero-dimensional, one-dimensional, two-dimensional and three-dimensional nanostructured materials for advanced electrochemical energy devices. *Prog. Mater. Sci.* **2012**, *57*(4), 724–803. https://doi.org/10.1016/j.pmatsci.2011.08.003
2. Laurent et al., Title of the article. *Chem. Rev.* **2010**, *110*.
3. Dreaden, E.C.; Alkilany, A.M.; Huang, X.; Murphy, C.J.; El-Sayed, M.A. The golden age: Gold nanoparticles for biomedicine. *Chem. Soc. Rev.* **2012**, *41*(7), 2740–2779. https://doi.org/10.1039/c1cs15237h
4. Dreaden, E.C.; Alkilany, A.M.; Huang, X.; Murphy, C.J.; El-Sayed, M.A. The golden age: Gold nanoparticles for biomedicine. *Chem. Soc. Rev.* **2012**, *41*(7), 2740–2779. https://doi.org/10.1039/c1cs15237h.
5. Nowrouzi A.; Meghrazi K.; Golmohammadi T.; Golestani A.; Ahmadian S.; Shafiezadeh M.; Shajary Z.; Khaghani S.; Amiri A.N. Cytotoxicity of subtoxic AgNP in human hepatoma cell line (HepG2) after long-term exposure. *Iran. Biomed. J.* **2010**, *14*(1-2), 23–32.
6. De Berardis B.; Civitelli G.; Condello M.; Lista P.; Pozzi R.; Arancia G.; Meschini, S. Exposure to ZnO nanoparticles induces oxidative stress and cytotoxicity in human colon carcinoma cells. *Toxicol. Appl. Pharmacol.* **2010**, *246*(3), 116–127.
7. Vishwakarma V.; Samal S.S.; Manoharan N. Safety and risk associated with nanoparticles-a review. *J. Minerals Mater. Charact. Eng.* **2010**, *9*(5), 455.
8. Yang L.; Watts D.J. Particle surface characteristics may play an important role in phytotoxicity of alumina nanoparticles. *Toxicol. Lett.* **2005**, *158*(2), 122–132.
9. Mostafalou S.; Mohammadi H.; Ramazani A.; Abdollahi M. Different biokinetics of nanomedicines linking to their toxicity; an overview. *Daru J. Pharm. Sci.* **2013**, *21*(1), 14.
10. Oberdörster G.; Oberdörster E.; Oberdörster J. Nano-toxicology: An emerging discipline evolving from studies of ultrafine particles. *Environ. Health Perspect.* **2005**, *113*(7), 823–839.
11. Tucker, N.; Stanger, J.J.; Staiger, M.P.; Razzaq, H.; Hofman, K. The history of the science and technology of electrospinning from 1600 to 1995. *J. Eng. Fibers Fabr.* **2012**, *7*(2_suppl), 155892501200702S10.
12. Aman Mohammadi, M.; Hosseini, S.M.; Yousefi, M. Application of electrospinning technique in development of intelligent food packaging: A short review of recent trends. *Food Sci. Nutr.* **2020**, *8*(9), 4656-4665.
13. Kim, H.H.; Park, Y.H.; Yoon, K.J.; Kim, K.O. Fabrication of nanofibrous silkworm gland three-dimensional scafold containing micro/nanoscale pores and study of its efects on adipose tissue-derived stem cell growth. *J. Mater. Sci.* **2016**, *51*, 9267–9278.
14. Kim, K.O.; Akada, Y.; Kai, W.; Kim, B.S.; Kim, I.S. Cells attachment property of PVA hydrogel nanofibers incorporating hyaluronic acid for tissue engineering. *J. Biomater. Nanobiotechnol.* **2011**, *2*, 353–360.
15. Park, J.C.; Ito, T.; Kim, K.O.; Kim, K.W.; Kim, B.S.; Khil, M.S.; Kim, H.Y.; Kim, I.S. Electrospun poly (vinyl alcohol) nanofibers: effects of degree of hydrolysis and enhanced water stability. *Polymer J.* **2010**, *42*(3), 273–276.
16. Saallah, S.; Naim, M.N.; Lenggoro, I.W.; Mokhtar, M.N.; Bakar, N.F.A.; Gen, M. Immobilisation of cyclodextrin glucanotransferase into polyvinyl alcohol (PVA) nanofibres via electrospinning. *Biotechnol. Rep.* **2016,** *10*, 44–48.
17. Kim, G.J.; Yoon, K.J.; Kim, K.O. Glucose-responsive poly (vinyl alcohol)/β-cyclodextrin hydrogel with glucose oxidase immobilization. *J. Mater. Sci.* **2019**, *54*, 12806–12817.
18. Kharaghani, D.; Gitigard, P.; Ohtani, H.; Kim, K.O.; Ullah, S.; Saito, Y.; Khan, M.Q.; Kim, I.S. Design and characterization of dual drug delivery based on in-situ assembled PVA/PAN core-shell nanofibers for wound dressing application. *Sci. Rep.* **2019**, *9*(1), 12640. https://doi.org/10.1038/s41598-019-49132 (2019)
19. Kim, G.J.; Kim, K.O. Novel glucose-responsive of the transparent nanofiber hydrogel patches as a wearable biosensor via electrospinning, *Sci. Rep.* **2020**, *10* (1), 18858.
20. Wei, K.; Kim, K.O.; Song, K.H.; Kang, C.Y.; Lee, J.S.; Gopiraman, M.; Kim, I.S. Nitrogen-and oxygen-containing porous ultrafine carbon nanofiber: a highly flexible electrode material for supercapacitor, *J. Mater. Sci. Technol.* **2017**, *33*(5), 424–431.
21. Kim, K.O.; Kim, G.J.; Kim, J.H. A cellulose/β-cyclodextrin nanofiber patch as a wearable epidermal glucose sensor. *RSC Adv.* **2019**, *9*(40), 22790-22794.

22. Kim, K.O.; Kim, B.S.; Lee, K.H.; Park, Y.H.; Kim, I.S. Osteoblastic cells culture on electrospun poly (ε-caprolacton) scaffolds incorporating amphiphilic PEG–POSS telechelic. *J. Mater. Sci.: Mater. Med.* **2013,** *24*, 2029–2036.
23. Kim, K.O.; Kim, B.S. Immobilization of glucose oxidase on a PVA/PAA nanofiber matrix reduces the effect of the hematocrit levels on a glucose biosensor. *J. Fiber Sci. Technol.* **2017**, *73*(1), 27–33.
24. Lee, S.J.; Yoo, J.J.; Lim, G.J.; Atala, A.; Stitzel, J. In vitro evaluation of electrospun nanofiber scaffolds for vascular graft application. *J. Biomed. Mater. Res. A* **2007**, *83*(4), 999–1008.
25. Gomes, S.R.; Rodrigues, G.; Martins, G.G.; Roberto, M.A.; Mafra, M.; Henriques, C.M.R.; Silva, J.C. In vitro and in vivo evaluation of electrospun nanofibers of PCL, chitosan and gelatin: A comparative study. *Mater. Sci. Eng. C* **2015**, *46*, 348–358.
26. Nakkala, J.R.; Yao, Y.; Zhai, Z.; Duan, Y.; Zhang, D.; Mao, Z.; Lu, L.; Gao, C. Dimethyl itaconate-loaded nanofibers rewrite macrophage polarization, reduce inflammation, and enhance repair of myocardic infarction. *Small* **2021**, *17*(17), 2006992.
27. Sadeghi-Soureh, S.; Jafari, R.; Gholikhani-Darbroud, R.; Pilehvar-Soltanahmadi, Y. Potential of Chrysin-loaded PCL/gelatin nanofibers for modulation of macrophage functional polarity towards anti-inflammatory/pro-regenerative phenotype. *J. Drug Delivery Sci. Technol*. **2020**, *58*, 101802.
28. Wilson, V.G. Growth and differentiation of HaCaT keratinocytes. *Epidermal Cells: Methods Protocol.* **2014**, 33–41.
29. Kong, L.; Smith, W.; Hao, D. Overview of RAW264. 7 for osteoclastogensis study: Phenotype and stimuli. *J. Cellular Mol. Med.* **2019**, 23(5), 3077–3087.
30. Park, J.; Kim, H.D.; Lee, S.H.; Kwak, C.H.; Chang, Y.C.; Lee, Y.C.; Chung, T.W.; Magae, J.; Kim, C.H. Ascochlorin induces caspase-independent necroptosis in LPS-stimulated RAW 264.7 macrophages. *J. Ethnopharmacol.* **2019**, *239*, 111898.
31. Twentyman, P.R.; Luscombe, M. A study of some variables in a tetrazolium dye (MTT) based assay for cell growth and chemosensitivity. *Br. J. Cancer* **1987**, *56*(3), 279–285.
32. Elashmawi, I.S. Effect of LiCl filler on the structure and morphology of PVDF films. *Mater. Chem. Phys.* **2008**, *107*(1), 96–100.
33. Ye, Y.U.N.; Jiang, Y.; Wu, Z.; Zeng, H. Phase transitions of poly (vinylidene fluoride) under electric fields. *Integr. Ferroelectr.* **2006**, *80*(1), 245–251.
34. Li, J.C.; Wang, C.L.; Zhong, W.L.; Zhang, P.L.; Wang, Q.H.; Webb, J.F. Vibrational mode analysis of β-phase poly (vinylidene fluoride). *Appl. Phys. Lett.* **2002**, *81*(12), 2223–2225.
35. Boccaccio, T.; Bottino, A.; Capannelli, G.; Piaggio, P. Characterization of PVDF membranes by vibrational spectroscopy. *J. Membrane Sci.*, **2002**, *210*(2), 315–329.